Effect of crystalline morphology on fatigue crack propagation in polyethylene

J. RUNT*, M. JACQ
*Department of Materials Science and Engineering, Polymer Science Program,
The Pennsylvania State University, University Park, Pennsylvania 16802, USA*

An investigation of the influence of crystalline morphology on fatigue crack propagation (FCP) resistance in a slightly branched polyethylene is presented. Various thermal histories have been utilized to generate samples with different crystalline microstructures and the samples were characterized thoroughly using standard methods. Estimation of tie molecule densities was obtained from measurements of brittle fracture stress. Differences in FCP behaviour for the quenched and annealed samples were shown to be dictated by a competing effect between the degree of crystallinity and tie molecule density. Further, larger spherulite size and distribution appeared to have a deleterious effect on fatigue properties. In general, crystalline microstructure is shown to have a significant influence on fatigue crack propagation behaviour.

1. Introduction

The dynamic fatigue behaviour of semi-crystalline polymers has been under active investigation for many years [1, 2]. However, the emphasis has generally been on the effect of external variables such as stress amplitude and mean stress, test frequency and environmental media on fatigue behaviour. Even though crystalline morphology is generally recognized as playing a dominant role in controlling mechanical behaviour, very little research on the effect of morphology on fatigue has been conducted [2–4]. By morphology, we mean parameters such as the degree of crystallinity (w_c), spherulite size (D), lamellar thickness (L), and tie molecule density. In this paper, we report the results of our investigation of the influence of semi-crystalline morphology on fatigue crack propagation (FCP) in a lightly branched polyethylene (PE). Using various simple heat treatments, we were able to generate samples with very distinct crystalline morphologies and exhibiting different FCP behaviour.

2. Experimental details

The polymer used in this study was a polyethylene–hexene copolymer supplied by Phillips Chemical Company (Bartlesville, Oklahoma, USA), having a reported $M_W = 64\,000\,\mathrm{g\,mol^{-1}}$, $M_N = 17\,000\,\mathrm{g\,mol^{-1}}$, a density of $0.95\,\mathrm{g\,cm^{-3}}$ and 0.5% branches per mole. The polymer was first compression moulded at 200° C and 10 000 psi ($\sim 68.9\,\mathrm{N\,mm^{-2}}$) into the desired dimensions, then quenched into cold water.

2.1. Thermal history

Three different types of thermal treatments were used to generate samples with different microstructures. The first series of specimens was annealed in a silicone oil bath for 24 h at temperatures varying between 116 and 126° C, to achieve an increase in crystallinity with-

out affecting the supermolecular structure. The second set of samples was remelted at 160° C for 90 min before crystallization at a temperature between 120 and 126° C for 24 h. Variation of the crystallization temperature is considered to affect the supermolecular morphology. The last series was isothermally crystallized at 120° C after receiving different melt treatments to alter the spherulite size separately without affecting the other microstructural parameters, as suggested in the literature [5, 6]. These melt treatments were: melt at either 155 or 200° C for 90 min, or melt at 200° C for 90 min then quench to a second melt temperature of 155° C and maintain at this temperature for 90 min.

2.2. Morphological characterization

The crystalline morphology of the different specimens was characterized by various means. Heats of fusion and melting points were determined using a 7 series Perkin–Elmer differential scanning calorimeter. A heating rate of 20° C min^{-1} was used to obtain the melting endotherms of thin sections cut from the bulk (using a Reichert–Jung ultracut E microtome equipped with a glass knife). Baselines defining the endothermal area were drawn from 95 to 145° C and percentage crystallinities were calculated from the measured heats of fusion using 70 cal g^{-1} ($\sim 293\,\mathrm{J\,g^{-1}}$) as the heat of fusion of the 100% crystalline phase of PE. A minimum of two samples (sample weight approximately 2 to 3 mg) were run to determine the heat of fusion of each specimen type. Lamellar thicknesses (L) were not measured directly but estimated from the observed T_m obtained on thin samples ($\sim 8\,\mu m$) of weight between 0.4 and 0.8 mg, in combination with the Hoffman–Weeks equation [7], using 90 erg cm^{-2} ($9 \times 10^{-6}\,\mathrm{J\,cm^{-2}}$) for the end surface free energy and 141° C as the equilibrium melting point.

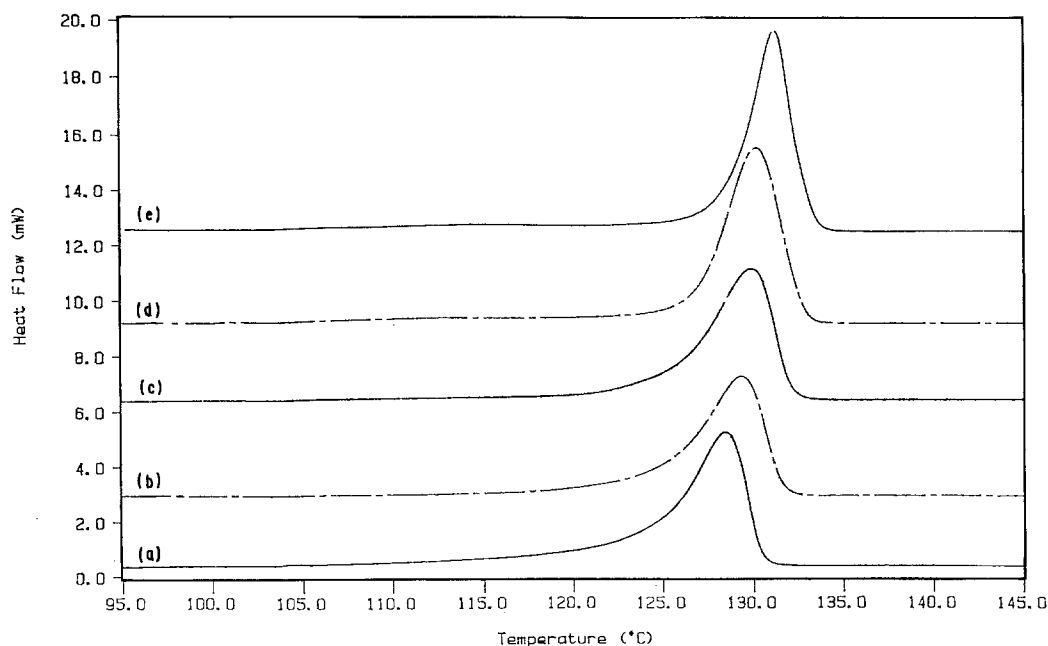Spherulite sizes (D) and texture were monitored

---

Figure 1 DSC thermograms: (a) quenched sample, and sample annealed at (b) 116°C, (c) 119°C, (d) 123°C, (e) 126°C.

under crossed polarizers with an Olympus BHSP-300 optical microscope equipped with a PM-10AD photomicrographic system. For spherulitic superstructures, the maximum spherulite size on the photomicrographs was used as an estimate of the spherulite size distribution. Spherulite morphology was also monitored using low-angle laser light scattering. The light scattering was conducted under crossed polars (Hv scattering) using a Model 1460 optical multichannel analyser, equipped with a two-dimensional position-sensitive vidicon detector, 1216 multichannel detector controller and a DMP-40 plotter.

The tie molecule density was not measured directly but evaluated from brittle fracture stress measurements as suggested by Brown and Ward [8]. Our purpose is not to obtain precise quantitative measurement of the tie molecule density but rather qualitative information which will permit a comparison and ranking of the various samples. The brittle fracture stress of dogbone-shaped specimens was determined on an Instron testing machine at − 120° C and a cross-head speed of 50 cm min^{-1}. In their publication, Brown and Ward proposed a model which allows one to estimate the area fraction of tie molecules, f_T (defined as the fraction of the interlamellar area covered by tie molecules) from the measured brittle

fracture stress. It is assumed that the brittle fracture stress (σ_B) is equal to the sum of the strength derived from the tie molecules and the van der Waals' bonds in the interlamellar area. The area fraction of tie molecules, f_T, is given by

$$f_T = (C\sigma_B - \beta E_{iso})/\beta(E_T - E_{iso}) \qquad (1)$$

where E_T is the Young's modulus of the tie molecules, E_{iso} the Young's modulus for the van der Waals' bonds, β a constant of proportionality and C a stress concentration factor. The following values were used in our calculations and come from those proposed by Brown and Ward: 300 GPa for the Young's modulus of the tie molecules, 8 GPa for the Young's modulus of the van der Waals' bonds, 0.1 for the constant of proportionality and 50 for the stress concentration.

2.3. Mechanical properties

All room-temperature tensile experiments were conducted at a cross-head speed of 10 cm min^{-1} on an Instron Table Model Universal Testing Instrument (TM-S). The gauge length was 3/4 in. ($\sim$ 1.9 cm) for all samples. A minimum of five samples of each specimen type was tested and the standard deviation associated with each derived parameter was calculated.
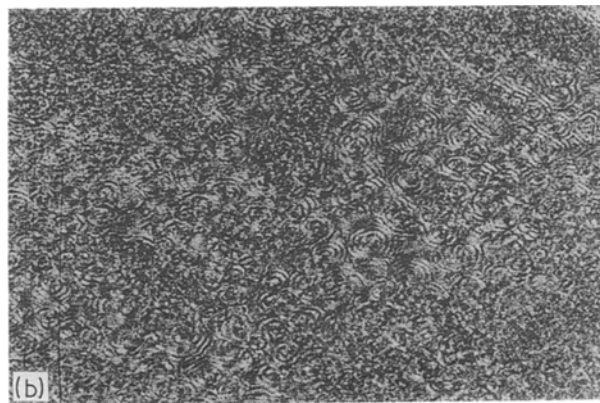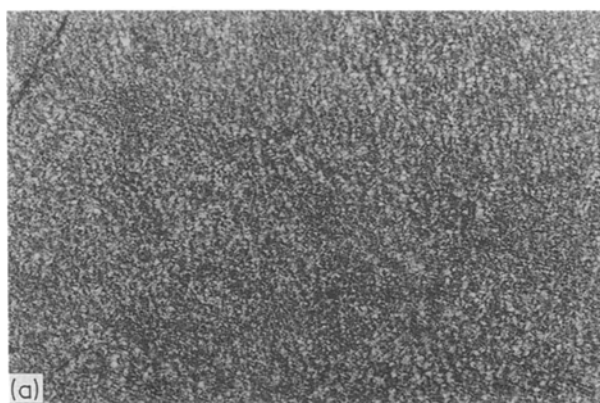
All fatigue experiments were performed on an

Figure 2 Optical micrographs: (a) quenched sample, (b) sample crystallized at 120° C.
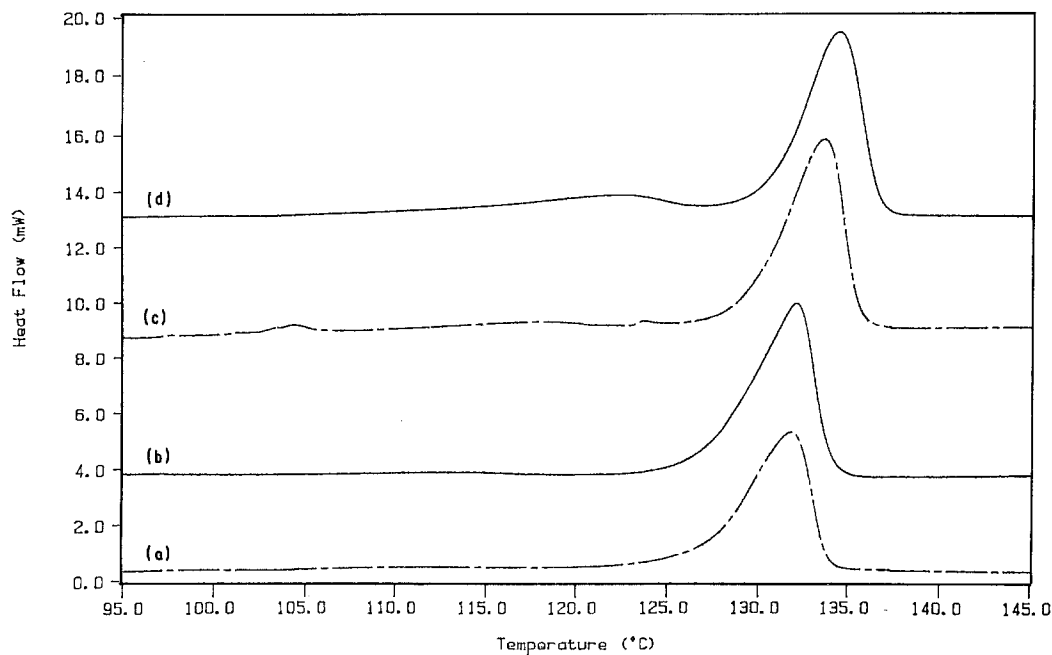
Figure 3 DSC thermograms of the samples crystallized at (a) 120°C, (b) 122°C, (c) 124°C, (d) 126°C.

Instron servohydraulic testing machine model 1331, equipped with a 2500 lb ($\sim$ 1133.9 kg) load cell. Compact-tension shaped specimens with dimensions of 2.45 in. by 2.3 in. by 0.25 in. thick ($\sim$ 6.2 cm × 5.8 cm × 0.6 cm) were used in all experiments. Notches approximately 1 in. (2.54 cm) long were cut into each sample with a hacksaw. The notch tip was then sharpened with a razor blade. A new razor blade was used for each sample. Samples were cracked in tension-compression at 1 Hz to minimize heat generation at the crack tip. Experiments were conducted in load control using a sinusoidal waveform of constant mean stress of 14.5 lb ($\sim$ 6.6 kg). The load ratio was kept constant within each series of samples, but changed slightly from the quenched and annealed ($\sim$ −0.11) to the isothermally crystallized ones ($\sim$ −0.07) due to the somewhat lower load amplitude required to generate cracks propagating at a sufficiently low rate to permit recording of the data. Crack length was monitored with a Gaertner travelling microscope. The stress concentration factor at the crack tip (K) for a compact tension specimen is given as a function of the applied load (L), the specimen dimensions and a geometrical factor, Y (defined in the ASTM D671) in the following equation

$$K = Y (L/BW^{1/2}) \qquad (2)$$

where B is the thickness and W the width as defined in ASTM D671. Plots of da/dN (the crack propagation rate) against ΔK are used to compare the fatigue behaviour obtained from different samples.

Fracture surfaces were analysed in order to understand further the nature of the deformation mechanism involved during crack propagation. This work was conducted with an ISI-SX-40 scanning electron microscope. All surfaces were previously stained by ruthenium tetraoxide vapour. Further details on the procedure can be found in [9].

3. Results and discussion
3.1. Characterization
Microstructural data of the quenched and annealed specimens are reported in Table I. Within this series of samples, an increase in the degree of crystallinity and melting point (lamellar thickness) is observed with increasing annealing temperature. Representative differential scanning calorimetry (DSC) thermograms of the different specimens are illustrated in Fig. 1. All samples exhibit an identical spherulitic structure, with an average diameter of 5 μm and a maximum size of 35 μm, as can be observed in Fig. 2a.

Table II lists the various morphological information obtained on the isothermally crystallized samples. No significant variation in crystallinity was observed between the different specimens. An increase in melting point (and lamellar thickness) was recorded with increasing crystallization temperature.

Fig. 3 shows the DSC thermograms of these samples. Non-spherulitic morphologies were observed in samples crystallized at temperatures of 122°C or higher. This compares to the situation for high-density PE where a temperature of 127°C has been reported [7] as the crystallization temperature associated with

TABLE I Microstructural characterization of the quenched and annealed samples

T_a of sample (°C)	W_c (%)	T_m (°C)	D (μm)	L (nm)
Quenched	57	128.5	5 (max 35)	20
116	60	129.3	5 (max 35)	22
119	62	129.9	5 (max 35)	23
123	64	130.2	5 (max 35)	24
126	64	131.3	5 (max 35)	26

TABLE II Microstructural characterization of the isothermally crystallized samples

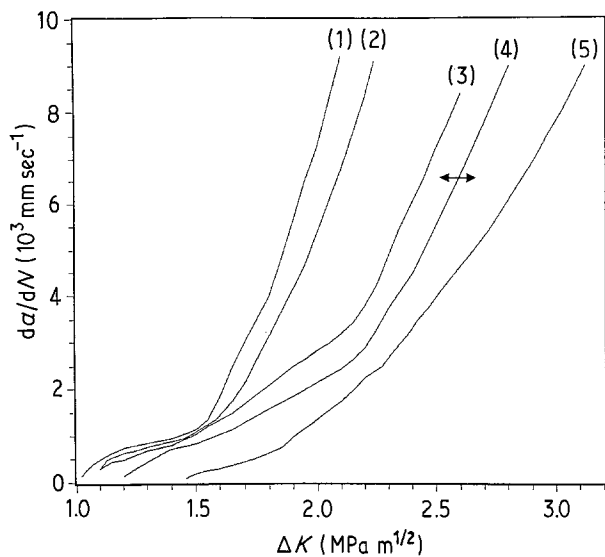| T_c of sample (°C)	W_c (%)	T_m (°C)	D (μm)	L (nm)
120	64	131.6	6.5 (max 95)	27
122	65	132.2	–	29
124	65	133.6	–	34
126	66	134.4	–	39

Figure 4 Plots of d*a*/d*N* against Δ*K* for the quenched and annealed samples. T_a = (1) 116°C, (2) 119°C, (3) 123°C, (4) quenched, (5) 126°C.

Figure 5 Plots of d*a*/d*N* against Δ*K* for the isothermally crystallized samples. T_c = (1) 120°C, (2) 122°C, (3) 124°C, (4) 126°C.

the transition from a spherulitic to non-spherulitic morphology and a change from regime 2 to regime 1 crystallization kinetics.

Variation of the spherulite size in a control manner without affecting other microstructural parameters was not possible with the techniques used here. All samples crystallized at 120°C exhibited the same spherulitic structure regardless of the melt treatment used, with an average spherulite size of 6.5 μm and a maximum diameter of 95 μm (see Fig. 2b). While only a small increase in the average spherulite size is obtained in these samples compared to the annealed ones, a larger maximum size was measured which may indicate a wider distribution.

3.2. Tensile testing

The room-temperature tensile properties of all samples can be found in Table III (σ_y and σ_B refer to the yield and tensile strength, respectively). The quenched and annealed samples have, within experimental error, similar tensile properties except for the elongation at break (ε_B) which shows a large decrease with increasing annealing temperature (from ∼400% to ∼100%). As far as the isothermally crystallized samples are concerned, all specimens have a similar modulus which is also equivalent, within experimental error, to those obtained for the quenched and annealed samples. Samples crystallized at 124 and 126°C failed in a brittle manner at the cross-head speed used in this
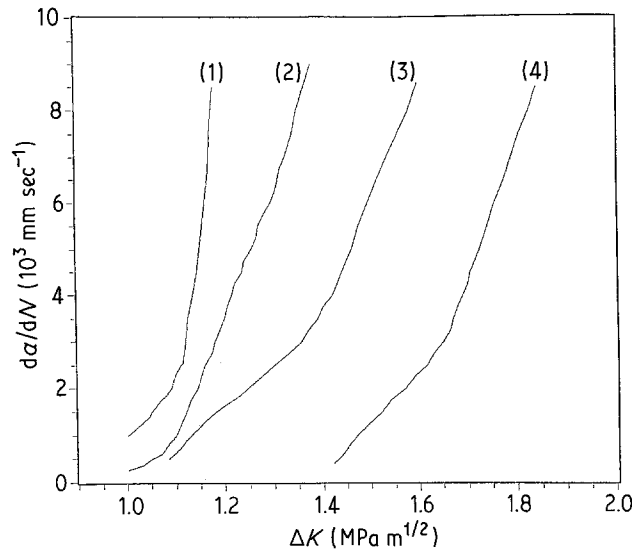
study. A significant increase in tensile strength as well as a decrease in ε_B was observed with increasing crystallization temperature.

3.3. Fatigue crack propagation results

The fatigue crack propagation behaviour of the quenched and annealed samples is illustrated in Fig. 4. The experimental error obtained from several runs is represented by a bar on the plot. Focusing initially on the four annealed samples, one first notices that annealing at progressively higher temperatures shifts the curves along the Δ*K* axis indicating an improvement of fatigue resistance. As mentioned previously, the spherulitic morphology remains constant on annealing. However, the degree of crystallinity increases and apparently accounts for the improvement in fatigue resistance. Because one would expect more energy to be required to deform a unit volume of material the higher the degree of crystallinity, this result seems reasonable. Considering the quenched sample, one realizes that it exhibits a higher resistance toward fatigue crack propagation than most of the annealed ones, although it has a lower degree of crystallinity. This indicates that other parameters influencing fatigue resistance also change during annealing. One possible explanation may be different tie molecule densities, because this is expected to decrease upon annealing [10]. Experimental values of the brittle fracture stress and estimated tie molecule density from Equation 1 are reported in Table IV.

TABLE III Tensile properties of the various samples

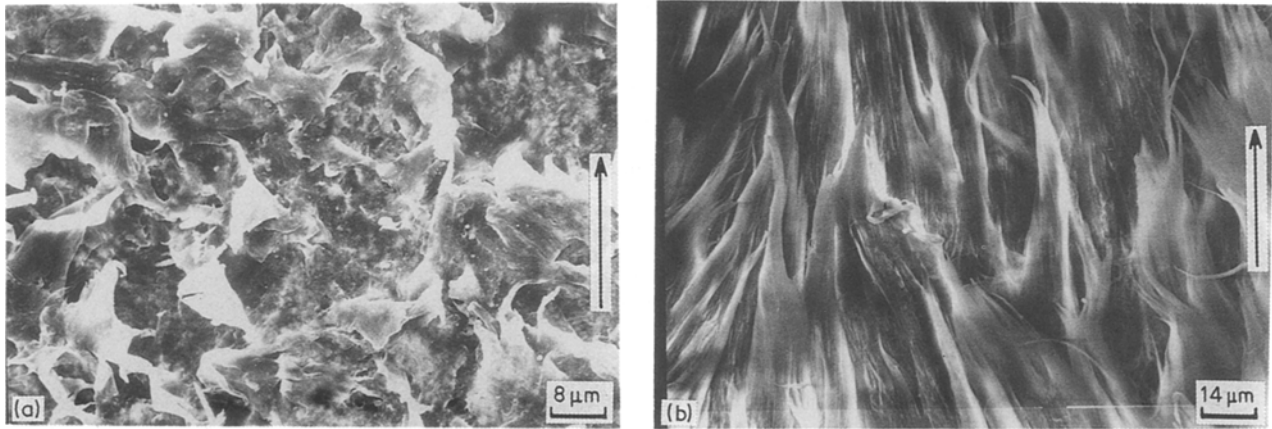|	Sample								
	Quenched	T_a (°C)				T_c (°C)			
		116	120	123	126	120	122	124	126
Modulus (MPa)	350 ± 8	350 ± 13	352 ± 7	347 ± 19	340 ± 13	338 ± 13	337 ± 33	362 ± 45	357 ± 38
σ_y (MPa)	24 ± 0.6	23.5 ± 0.5	24 ± 0.6	23.5 ± 0.4	24.5 ± 0.8	27.4 ± 4.4	30 ± 6.5	–	–
σ_B (MPa)	11.7 ± 0.3	10.8 ± 0.1	11.2 ± 0.5	10.8 ± 0.3	10.8 ± 0.3	19.1 ± 4.5	20.5 ± 3.8	25.8 ± 4.2	31.6 ± 7.1
ε_B (%)	472 ± 72	296 ± 41	267 ± 37	205 ± 68	117 ± 17	46 ± 31	33 ± 11	8.5 ± 0.6	11.2 ± 3.4

Figure 6 Fracture surface of the quenched sample (a) in the region of slow crack growth, (b) in the region of more rapid crack growth.

Values of f_T for the annealed samples tend to group around a similar value. On the contrary, the quenched sample has a calculated tie molecule density about twice that of the annealed samples. This indicates that while annealing the quenched sample significantly decreases the number of tie molecules in our polymer, this decrease is not much affected by the temperature of annealing. Going back to the FCP results, the decrease in tie molecule density appears to be responsible for the lower fatigue resistance of the sample annealed at 116° C, compared to the quenched one, despite its higher degree of crystallinity. However, a more severe annealing treatment increases the crystallinity without significantly affecting the tie molecule density. This is consistent with the gain in fatigue resistance observed for the other annealed samples. Eventually, the increase in crystallinity compensates for the decrease in tie molecule density.

Representative FCP curves of the isothermally crystallized samples are illustrated in Fig. 5. An increase in fatigue resistance is obtained with increasing crystallization temperature, even though there is no noticeable increase in crystallinity and that the tie molecule density is expected to decrease [11]. Thus, within this series of samples, the fatigue behaviour is opposite to the initial expectation. However, the experimental values obtained from measurements of the brittle fracture stress indicate that the tie molecule density changes in a random manner between the different samples (Table V) and it appears that the differences in fatigue behaviour cannot be explained by this parameter. The tie molecule densities of this series of samples appear, in general, to be somewhat lower than those of the annealed specimens and can account for the overall lower fatigue resistance as compared to the quenched and annealed ones (note

the different scales used in Figs 4 and 5). At this point, although there is no clear explanation for the differences in fatigue behaviour within the isothermally crystallized series, several suggestions can be raised. For example, an increase in crystalline perfection, usually thought to accompany crystallization at higher temperature, and changes in supermolecular structures may render the material more resistant to crack propagation.

As a spherulitic material, the sample crystallized at 120° C can be analysed along with the first series. In particular, it can be compared with the specimen annealed at 126° C because, besides the spherulite size and distribution, both samples possess similar microstructural characteristics. This comparison illustrates that differences in spherulitic morphology generated by different crystallization conditions can have a rather important influence on the FCP resistance considering the large difference in ΔK recorded between the two specimens. The observed loss of resistance is presumably due to the increase in spherulite size and distribution and, possibly, to a somewhat lower tie molecule density. This is consistent with the usual effect of spherulite morphology on various mechanical properties reported in the literature, where a larger spherulite size and distribution were found to have a deleterious effect [12, 13].

3.4. Fracture surface analysis

Macroscopically, the fracture surfaces of the specimens exhibit a semi-brittle character with almost no visible deformation. However, they display distinct features when examined microscopically. Two different types of deformation pattern can be observed on each fracture surface. At the beginning of slow crack propagation, one notices a regular surface with no apparent orientation of the deformed material

TABLE IV Brittle fracture stress and estimated area fraction of tie molecules of the quenched and annealed samples

	Sample				
	Quenched	T_a (° C)			
		116	120	123	126
Stress at break (MPa)	27.3	21.4	20.1	22.7	21.2
f_T	~ 0.019	~ 0.010	~ 0.007	~ 0.011	~ 0.009

TABLE V Brittle fracture stress and estimated area fraction of tie molecules of the isothermally crystallized samples

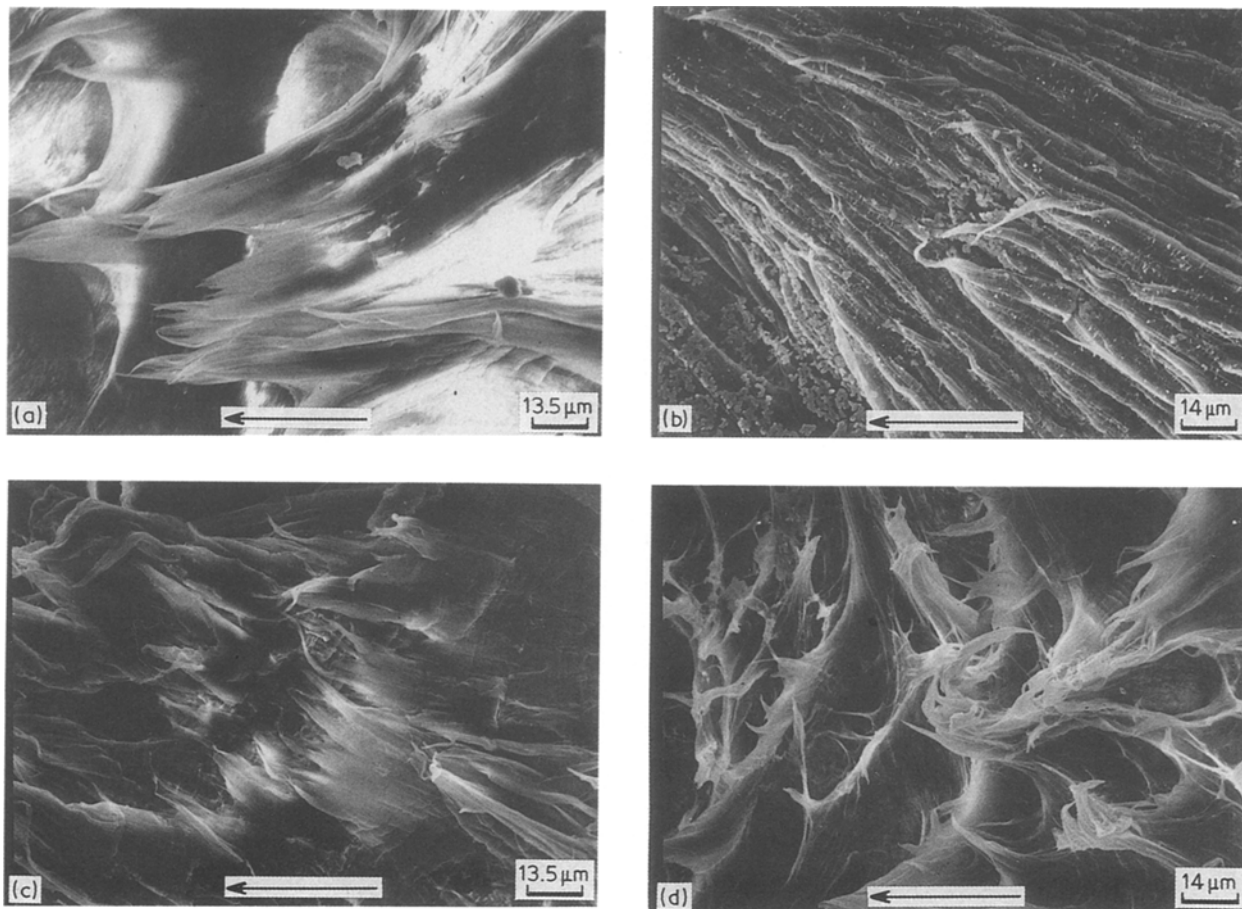|	T_c of sample (° C)			
	120	122	124	126
Brittle fracture stress (MPa)	19.5	20.9	18.4	21.1
f_T	~ 0.006	~ 0.008	~ 0.004	~ 0.008

Figure 7 Fracture surface in the region of more rapid crack growth of the sample annealed at (a) 116°C, (b) 119°C, (c) 123°C, (d) 126°C.

along the crack propagation direction. Second, a much more plastically-deformed area is observed which represents the deformation due to the more rapid crack growth when the crack is accelerating before catastrophic failure. All micrographs of the region of slow crack growth in the quenched and annealed samples exhibit the same features indicating that the deformation processes are similar for all samples. An example of such a micrograph taken from a quenched specimen is reported in Fig. 6a. The pattern exhibited in the region of more rapid crack growth revealed a fibrillar texture in which the fibrils are aligned in the direction of crack propagation, as shown in Fig. 6b (the arrows indicate the direction of crack propagation). Similar micrographs can be found in the literature (e.g. [14]). The fibrous nature of the surface has been associated with the formation of a crazed damage zone which precedes the crack. This indicates that crazing is at least partly involved in the deformation during fatigue crack propagation experiments of our polymer as well. As the annealing temperature increases, the fibres appear less drawn and the lengths of the fibrils become shorter, characteristic of less ductile failure (Fig. 7). This is consistent with the lower tensile elongation at break at higher annealing temperature observed in the simple load–elongation experiments.

The surfaces in the region of slow crack growth of the samples crystallized at 120, 122 and 124°C are identical to those of the quenched and annealed samples but with slightly less pronounced plastic

deformation. On the other hand, the sample crystallized at 126°C exhibits a surface more indicative of brittle fracture with no indication of deformation as shown in Fig. 8. Micrographs in the region of rapid crack growth of all samples indicate the formation of voids and fibrils during plastic deformation but with almost no orientation of the fibrils (Fig. 9). The plastic deformation in this series of samples appears to occur through crazing as well. The lack of orientation of the fibres is consistent with the relatively brittle character of the samples expected on the basis of the tensile experiments.

Finally, note that within each series of samples, specimens having higher FCP resistance also exhibit
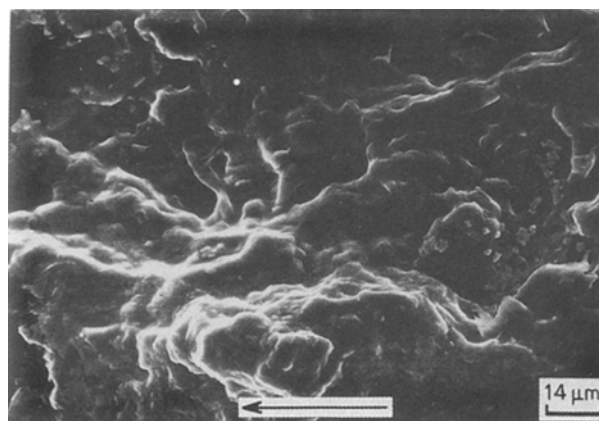

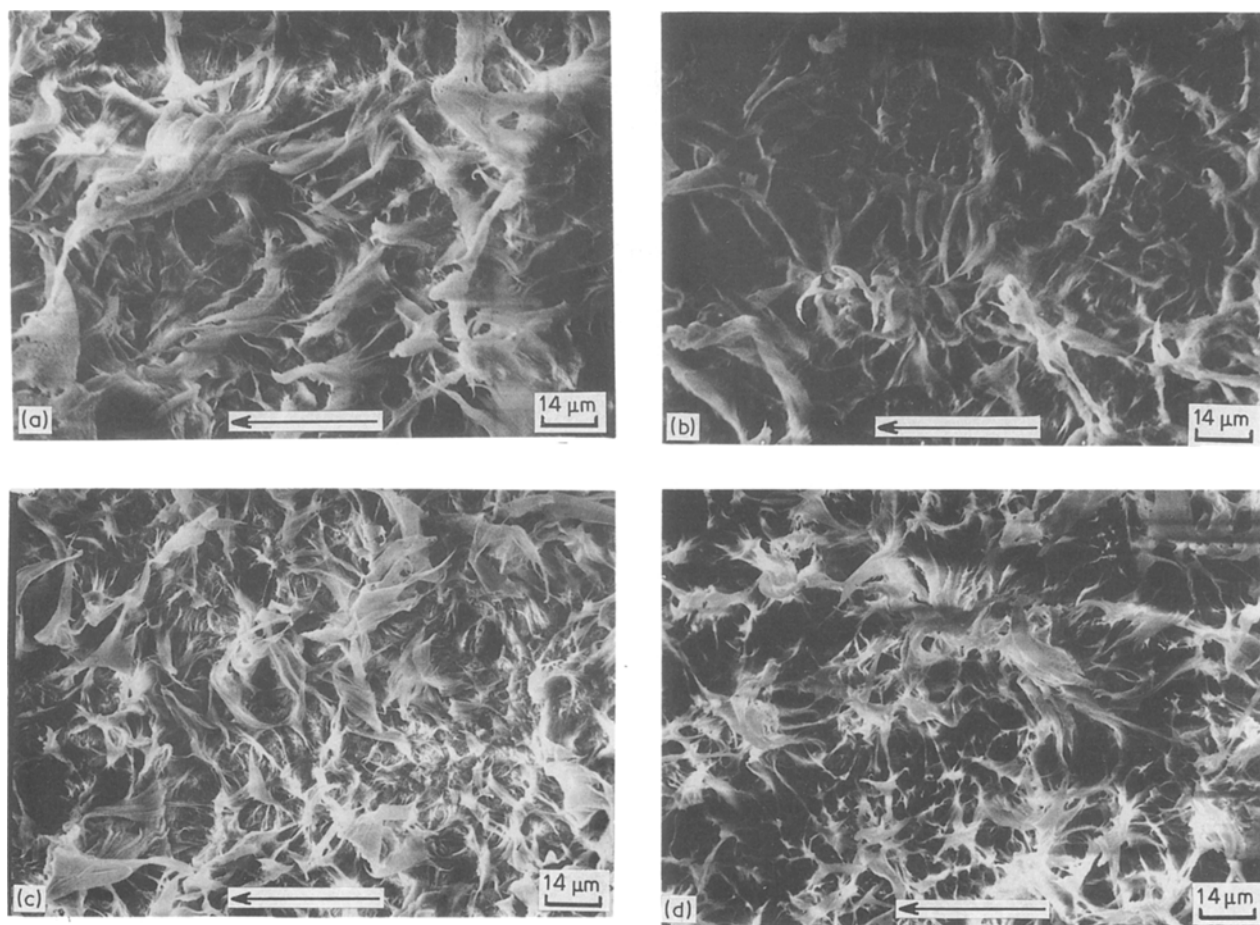*Figure 8* Fracture surface of the sample crystallized at 126°C in the region of slow crack growth.

1426

Figure 9 Fracture surface in the region of more rapid crack growth of the samples crystallized at (a) 120° C, (b) 122° C, (c) 124° C, (d) 126° C.

fracture surfaces indicating less plastic deformation (see Figs 7, 8 and 9), in contrast with our initial expectations. While the reason for this is still not clear, consideration of the total volume of material which is plastically deformed during crack propagation provides a possible explanation. The crack tip is surrounded by a three-dimensional plastic deformation zone and several models have been proposed to calculate the anticipated size and shape [1]. Starting with the Dugdale model and assuming a cylindrical deformation zone, a rough estimate of the volume ratio of the material expected to be plastically deformed for the sample annealed at 126° C to that at 116° C was calculated. The size of the deformation zone of the specimen annealed at 126° C was calculated to be roughly three to five times larger than for that annealed at 116° C and is consistent with the higher FCP resistance of the former specimen.

4. Conclusions

Variation in the degree of crystallinity without affecting the spherulite size was possible through an annealing treatment. While a decrease in tie molecule was measured between the quenched and annealed samples, this decrease was independent of the annealing temperature. A competing effect on FCP resistance between the increase in crystallinity during annealing and the resulting decrease in tie molecule density was observed.

An increase in fatigue crack propagation resistance with increasing crystallization temperature was observed although no noticeable differences in crystallinity were measured. Further, the estimated tie molecule density varies randomly between the various samples and does not appear to be responsible for the differences in FCP behaviour. However, tie molecule density appears to be slightly lower for this series of samples than for the quenched and annealed and probably accounts for the generally lower resistance of the isothermally crystallized specimens. The underlying reason for the improvement in fatigue crack propagation resistance with crystallization temperature is unclear at present but the general relationship between the isothermally crystallized samples (and annealed ones) may be rationalized by considering the total volume of material plastically deformed during crack propagation.

Even though variation of the spherulite size in a controlled manner was not possible, the effect of spherulite size and distribution has been separated by comparing the sample crystallized at 120° C with that annealed at 126° C. As expected, a larger spherulite size and distribution appears to have a deleterious effect on the fatigue crack propagation properties.

Acknowledgement

References

1. R. W. HERTZBERG and J. A. MANSON, in "Fatigue of Engineering Plastics" (Academic, New York, 1980).

2. J. A. MANSON and R. W. HERTZBERG, *Ency. Polym. Sci. Engng* 7 (1986) 379.
3. F. X. de CHARENTENAY, F. LAGHOUATI and J. DEWAS, in "Deformation, Yield and Fracture of Polymers" (Plastic and Rubber Institute, Cambridge, 1979) p. 61.
4. A. RAMIREZ, J. A. MANSON and R. W. HERTZBERG, *Polym. Engng Sci.* 22 (1982) 975.
5. T. I. SOGOLOVA, *Mekhan Polym.* 1(1965) 5.
6. L. W. KLEINER, M. R. RADLOFF, J. M. SCHULTZ and T-W. CHOU, *J. Polym. Sci. Polym. Phys. Edn* 12 (1974) 819.
7. J. D. HOFFMAN, G. T. DAVIS and J. I. LAURITZEN, in "Treatise on Solid State Chemistry", Vol. 3, edited by N. B. Hannay (Plenum, New York, 1975) p. 497.
8. N. BROWN and I. M. WARD, *J. Mater. Sci.* 18 (1983) 1405.
9. J. S. TRENT, *Macromol.* 17 (1984) 2930.
10. L. E. NIELSEN, "Mechanical Properties of Polymers and Composites" (Marcel Dekker, New York, 1974).
11. U. W. GEDDE and J. F. JANSSON, *Polymer* 26 (1985) 1469.
12. J. A. SAUER and G. C. RICHARDSON, *Int. J. Fract.* 16 (1980) 499.
13. J. L. WAY and J. R. ATKINSON, *J. Mater. Sci.* 6 (1971) 102.
14. A. LUSTIGER and R. D. CORNELIUSSEN, *ibid.* 22 (1987) 2470.